Stimulated four-photon nonlinear processes in few-mode glass-fiber optic waveguides

E. M. Dianov, É. A. Zakhidov, A. Ya. Karasik, P. V. Mamyshev, and A. M. Prokhorov

P. N. Lebedev Physics Institute, USSR Academy of Sciences

Stokes–anti-Stokes pairs with frequency shifts up to 550 cm^{-1} are obtained at the exit of a few-mode optic waveguide pumped by a neodymium garnet laser ($\lambda = 532$ nm). The optic emission is explained by assuming four-photon mixing and observance of the interacting-wave mode-locking conditions. On the basis of the investigation of the four-photon process, a technique is proposed and demonstrated for the measurement of the dispersion characteristics of optic waveguides. It is shown experimentally that the dispersion characteristics of fiber-optic waveguides with a germanium-doped silica core obtained by precipitation from the gas phase differ significantly from those of optic waveguides having an idealized steplike refractive-index profile. Measurement of only the frequency shift of the Stokes–anti-Stokes component suffices to determine an important parameter of the optic waveguide, viz., the ellipticity of the core. It is demonstrated experimentally that stable linearly polarized higher-order modes propagate in optic waveguides having cores of sufficiently small ellipticity.

PACS numbers: 42.80.Lt, 42.80.Mv, 42.65.Cq

I. INTRODUCTION

Glass-fiber optic waveguides (GFOW) have been attracting persistent attention as objects for the investigation of nonlinear processes. The high power densities in conjunction with the long duration of the interaction of the laser radiation with the medium have made it possible to increase substantially the efficiencies of such stimulated processes as stimulated Raman scattering (SRS) and stimulated Brillouin scattering (SBS), and to develop on their basis frequency-tunable sources of laser radiation. Nonlinear processes such as phase modulation, the optical Kerr effect, and others were investigated at very low intensities of the laser radiation in GFOW (see the review by Stolen[1]).

The presence of a nonzero real part of the third-order nonlinear susceptibility χ_3 in glass makes possible induced four-photon processes (SFPP), wherein two pump photons $\hbar\omega_{P1}$ and $\hbar\omega_{P2}$ are transformed into a Stokes ($\hbar\omega_S$) and an anti-Stokes ($\hbar\omega_A$) photons ($\omega_A > \omega_P > \omega_S$). The energy conservation law requires here

$$\omega_{P1} + \omega_{P2} = \omega_A + \omega_S.$$

The interacting-wave phase-locking conditions in SFPP are written for the wave vectors in the form

$$\mathbf{k}_{P1} + \mathbf{k}_{P2} = \mathbf{k}_A + \mathbf{k}_S; \quad k = 2\pi n/\lambda$$

(λ is the wavelength and n is the refractive index). In nonwaveguide media with normal material dispersion, in collinear interaction of plane waves, the mode-locking condition cannot be satisfied, inasmuch as we always have

$$\mathbf{k}_A + \mathbf{k}_S > \mathbf{k}_{P1} + \mathbf{k}_{P2}.$$

Mode locking in such media is reached when the waves interact at definite angles; the effective interaction length of these waves is small. In a waveguide medium, owing to the mode dispersion, mode locking at large interaction lengths can be obtained on account of the cancellation of the dispersion of the medium by the mode dispersion. This can be understood by imagining a situation in which photons with frequencies ω_P, ω_A, and ω_S propagate in different modes having different propagation constants.

Actually, stimulated four-photon processes in few-mode GFOW were analyzed and first observed under mode-locking conditions by Stolen, waveguide being excited by a neodymium laser.[2] The frequency shifts

$$\Delta\nu = \nu_A - \nu_P = \nu_P - \nu_S$$

in Ref. 2 were less than 400 cm^{-1}. IFPP were subsequently observed with large frequency shifts, several thousand cm^{-1}, in both multimode gradient GFOW[3] and in few-mode GFOE.[4,5] In a preceding paper[5] we reported observation of SFPP in a few-mode GFOW with maximum frequency shifts $\Delta\nu \sim 5000$ cm^{-1}.

Our present purpose was to investigate the influence of GFOW parameters such as the mode composition, the dispersion characteristics, the refractive-index profile, and the ellipticity of the core on the mode locking in SFPP, as well as an investigation of the possibility of developing frequency-tunable lasers based on SFPP in fiber optics.

II. EXPERIMENTAL PROCEDURE AND INVESTIGATED OBJECTS

The stimulated processes were observed by focusing the second harmonic of a Q-switched neodymium-garnet laser ($\lambda_P = 532$ nm), with a pulse-repetition frequency 12.5–25 Hz and pulse duration ~15 nsec, was focused by lens L_1 into the GFOW W (Fig. 1). Lenses with magnification from 3.7^x to 40^x were used. The pump power at which the SFPP was observed was limited by the damage to the input face of the GFOW. The measured values of the power at the output of the GFOW reached ~10 kW. To rotate the laser-radiation polarization, a half-wave phase plate ($\lambda/2$) was placed in front of the lens L_1. The radiation leaving the GFOW was passed through a polarization analyzer (Glan prism), and in certain cases through a quarter-wave phase plate ($\lambda/4$) onto a beam-splitting plate (BP), after
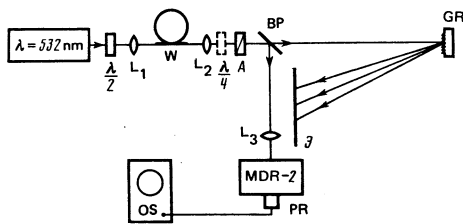
FIG. 1. Diagram of experimental setup.

which, part of the radiation was incident on a diffraction grating (Gr), and part was focused by lens L_3 onto the input slit of an MDR-2 grating monochromator. The signal from a photoreceiver placed behind the exit slit of the monochromator was recorded with an oscilloscope (OS). The radiation past the grating Gr was visually observed on a screen or photographed.

The investigated objects were two light guides with $SiO_2 + GeO_2$ core and SiO_2 cladding, obtained by the method of chemical precipitation from the gas phase from one of the same stock piece. GFOW Nos. 1 and 2 had respectively core diameters $2a \approx 9$ and 7.4 μm and cladding diameters $2d \approx 140$ and 150 μm. The difference between the refractive indices of the core and the cladding in both GFOW, which had the same refractive-index profile, was $\Delta n = n_1 - n_2 \approx 4.5 \cdot 10^{-3}$.

The calculated characteristic frequency parameter of the GFOW

$$V = 2\pi v a (n_1{}^2 - n_2{}^2)^{1/2}$$

at the pump wavelength $\lambda_P = 532$ nm was $V \approx 6$ and $V \approx 4.9$ for GFOW No. 1 and No. 2, respectively. Figure 2 shows plots of the normalized propagation constants b of certain linearly polarized LP_{lm} modes vs. the parameter V. These plots were calculated theoretically[6,7] for GFOW in the approximation $\Delta n = 0$. It can be seen from Fig. 2 that six modes will propagate in GFOW No. 1 at $V = 6$, and four modes in GFOW No. 2 at $V = 4.9$. The investigations were made on GFOW segments 0.3–10 m long.

III. EXPERIMENTAL OBSERVATION OF SFPP

As already mentioned, in Ref. 5 we have reported in particular, generation of Stokes–anti-Stokes (S–A) pairs obtained in GFOW No. 1, 6–10 m long, with small
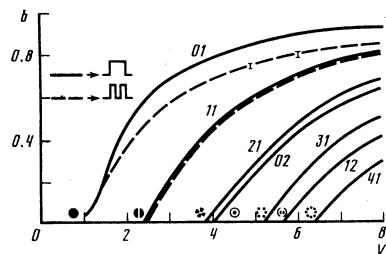

FIG. 2. Dependence of the normalized propagation constant b of LP_{lm} modes on the characteristic frequency parameter V for optic waveguides with different refractive-index profiles.[6,7] The figure shows also the near fields of the corresponding modes.

frequency shifts $\Delta v = v_A - v_P = v_P - v_S$ (of the order of hundreds of cm^{-1}). By varying the conditions under which the pump radiation enters the GFOW (for example, by measuring the entry angle of the radiation), we have observed in the lasing four combination Stokes–anti-Stokes pairs with different frequency shifts for each combination. The characteristic features of the observed processes (we shall call them SFPP with small frequency shifts) were the following. For each observed combination, first, the mode of the Stokes component differed from the mode of the anti-Stokes component; second, the Stokes component corresponded to a higher-order mode than the anti-Stokes component.

We observed in the experiment the following combinations in the generation of the Stokes–anti-Stokes pairs: 1) the Stokes component (S) corresponded to the LP_{11} mode and the anti-Stokes component (A) to the LP_{01} mode, with a measured frequency shift $\Delta v \approx 105$ cm^{-1}; 2) $S(LP_{21})$, $A(LP_{11})$, and $\Delta v \approx 110$ cm^{-1}; 3) $S(LP_{31})$, $A(LP_{21})$, and $\Delta v \approx 67$ cm^{-1}. In addition to these three combinations, we observed also generation of a Stokes component $S(LP_{12})$ and a corresponding anti-Stokes component $A(LP_{01})$. The generation of this pair of modes, however, was unstable, because the LP_{12} mode is close to cutoff for this GFOW (Fig. 2), and is poorly guided by the fiber.

All of the observed SFPP with small frequency shifts are characterized by the somewhat higher radiation intensity of the Stokes components compared with the intensity of the anti-Stokes components. This fact, at these frequency shifts, is apparently due to the nonzero imaginary part of the nonlinear third-order susceptibility, which is responsible for the SRS process.[8] (The spectrum of the spontaneous Raman scattering for fused quartz extends all the way to $\Delta v \sim 1000$ cm^{-1}, Ref. 1.) In fact, SRS was observed in the investigated GFOW and furthermore with somewhat larger values of the threshold pump power than for SFPP, on fiber segments of length shorter than 6 m. With increasing length of the fiber, the SRS process, which manifests itself in the fact that only Stokes components with $\Delta v \sim 460$ cm^{-1} are generated for the first component,[9] developed more effectively than the SFPP. Notice should also be taken of a certain frequency "smearing" of the Stokes–anti-Stokes components, which is apparently due to variation of the fiber diameter over its length.

Figure 3 shows photographs of the near field of the Stokes–anti-Stokes pair radiation, obtained with fibers 0.3–1 m long and with frequency shifts $\Delta v > 1000$ cm^{-1}. In Fig. 3 one can see generation of two Stokes–anti-Stokes pairs S_1–A_1 corresponding to LP_{11} modes, with the direction of the lobes of one Stokes–anti-Stokes pair ($\Delta v_1 \approx 1950$ cm^{-1}) perpendicular to the direction of the lobes of the second pair ($\Delta v_2 \approx 2100$ cm^{-1}) (GFOW No. 1). For GFOW No. 2, we observed the same picture, but with different frequency shifts, $\Delta v_1 \approx 2600$ and Δv_2 2800 cm^{-1}. The pump power corresponding to threshold value of the lasing of these pairs, measured at the output of GFOW No. 1 of ~0.6 m length was ~1 kW. We observed also generation of
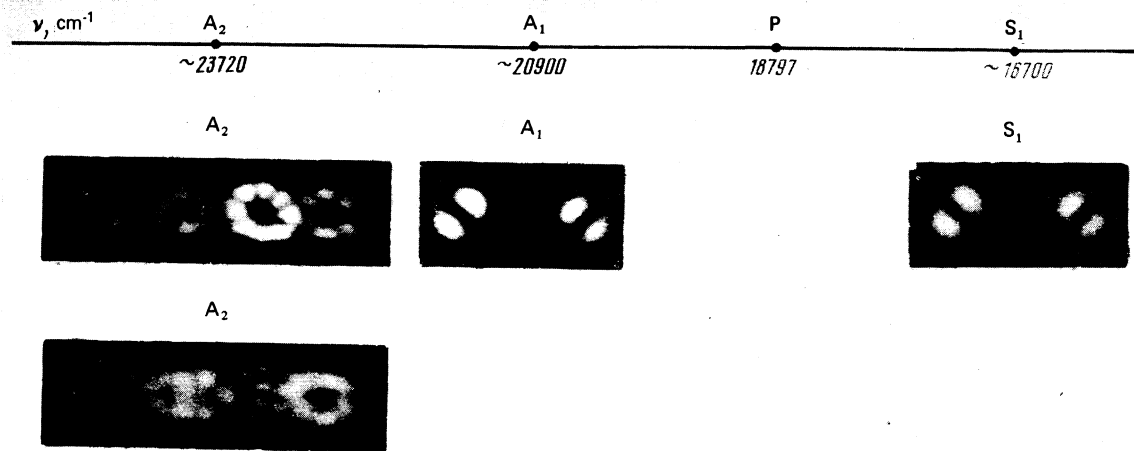
~23720   ~20900   18797   ~18700

FIG. 3. Photographs of the SFPP radiation at the exit from optic waveguide No. 1 of length ~0.6 m after diffraction by a grating. P, A, and S correspond to the near field of the pump radiation and of the anti-Stokes and Stokes components. The photograph S$_1$ was mistakenly rotated through 180°.

Stokes–anti-Stokes mode with even larger values of $\Delta\nu$. The maximum frequency shift for GFOW No. 1 was $\Delta\nu \approx 4940$ cm^{-1} ($\lambda_A \simeq 421.5$ nm, $\lambda_s \approx 721$ nm). For GFOW No. 2 the corresponding value was $\Delta\nu \approx 5500$ cm^{-1}. Figure 3 (A$_2$) shows generation in the anti-Stokes region for GFOW No. 1. It is seen that sets of 4–6 modes, spread over the spectrum, participate simultaneously in the generation. It is of interest to note that the modes LP_{22} and LP_{44} participate in the generation, even though they do not propagate in this GFOW at the pump wavelength (532 nm), by virtue of the cutoff condition (Fig. 2).

All the observed generated mode in the SFPP with small and large frequency shifts, in both the Stokes and anti-Stokes regions, were depolarized (this was verified with the aid of the $\lambda/4$ plate and the analyzer A, see Fig. 1), regardless of the azimuth of the linear polarization of the pump, which could be smoothly varied with the aid of the $\lambda/2$ plate.

IV. MODE LOCKING IN FOUR-PHOTON PROCESSES

The propagation constant of a linearly polarized LP_{lm} of an optic waveguide is given by[6]

$$\beta_{lm}=2\pi\nu n_1-2\pi\Delta n(1-b_{lm})\nu. \tag{1}$$

Assuming that Δn of the optic waveguide does not depend on the wavelength, we write for the propagation constants of the anti-Stokes and Stokes waves and of the pump wave the following equation

$$\beta_A+\beta_S-\beta_{P_1}-\beta_{P_2}=2\pi[(n_A+n_S-2n_P)\nu_P$$
$$+(n_A-n_S)\Delta\nu]+\{2\pi\Delta n(b_A\nu_A+b_S\nu_S-b_{P_1}\nu_P$$
$$-b_{P_2}\nu_P)\}\equiv\Delta k(\Delta\nu)+f(\Delta\nu). \tag{2}$$

The term in the square brackets [which we designate $\Delta k(\Delta\nu)$] describes the material dispersion (n_P, n_A, and n_S are the refractive indices of the fiber core at the pump, anti-Stokes, and Stokes component frequencies, respectively.) The term in the curly brackets of $f(\Delta\nu)$ describes the mode dispersion (b_{P_1}, b_{P_2}, b_A, and b_S are the normalized propagation constants for the modes in

which the pump photons and anti-Stokes and Stokes component photons propagate at the corresponding frequencies). The mode locking condition corresponding to cancellation of the material dispersion by the mode dispersion takes the form

$$\Delta k(\Delta\nu)+f(\Delta\nu)=0. \tag{3}$$

We transform $f(\Delta\nu)$, expanding $b_A\nu_A$ and $b_S\nu_S$ in powers of $\Delta\nu$, neglecting the terms with $(\Delta\nu)^2$:

$$f(\Delta\nu)=2\pi\Delta n[(b_A+b_S-b_{P_1}-b_{P_2})\nu_P$$
$$+\left(\frac{d(b_AV)}{dV}-\frac{d(b_SV)}{dV}\right)\Delta\nu]. \tag{4}$$

Here $d(dB)/dV$ are the normalized group delays of the LP modes.[6]

Figure 4 shows the function $\Delta k(\Delta\nu)$ plotted for pure fused quartz from the data of Ref. 10. The small GeO$_2$ content (~3 mol.%) in the investigated optic fibers hardly changes the plot of Fig. 4, which we have used in our calculations.

In the analysis of the experimental data with the aid of expressions (1)–(4) we made use of the dependences of the normalized phase constants b_{lm} of the different modes on the characteristic frequency parameter V (see Fig. 2) obtained for optic waveguides in the $\Delta n=0$ approximation. The solid lines in Fig. 2 are the curves obtained in Ref. 6 for optic
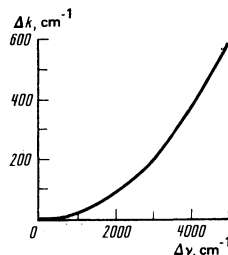

FIG. 4. Plot of the function $\Delta k(\Delta\nu)$, which describes the material dispersion for fused quartz [expression (2), $\lambda_P = 1/\nu_P = 532$ nm].

waveguides with stepwise distribution of the refractive-index profile. Real optic waveguides of germanium-doped quartz obtained by precipitation from the gas phase have at the center of the core a region with a decreased refractive index. In fact, this region is clearly seen in our optic fibers under a microscope, and the diameter of this region in the cross section of the fiber amounted in both investigated GFOW to ~1/4 of the diameter of the entire core (this was verified by photography, and densitometry of the cross section). The presence of such a region with decreased value of n manifests itself, for example, in a change of the intensity distribution in the near field of the LP_{0m} modes, whose fields for optical waveguides with step-like profiles of n have a maximum density at the center of the core. This fact was verified by us in experiment. In fact, the field of the LP_{01} at the center had a region with decreased intensity.

The presence of such a region with decreased n in the core of the optic fiber influences also its dispersion properties. Their change appears most strongly for the LP_{0m} modes and is significant to a lesser degree for LP_{lm} modes with $l \geqslant 1$, which have zero intensity at the center of the core. The dashed curves of Fig. 2 are plots of $b(V)$ for two modes, calculated in Ref. 7 for an optic waveguide with the profile shown in the same figure (the diameter of the region with decreased n is 0.25 of the diameter of the fiber core).

1. SFPP with small frequency shifts

As already noted in Sec. III of the present paper, the Stokes component in the observed SFPP with small frequency shifts the Stokes component always corresponds to a mode of higher order than the anti-Stokes component. Experiment shows then clearly that the pump corresponds to at least two modes. An analysis of expression (4) shows that the observed frequency shifts of ~100 cm^{-1} are possible only in the case if one pump photon propagates in the same mode as the Stokes photon, and the other pump photon in the mode together with the anti-Stokes photon. In this case expression (4) takes the form

$$f(\Delta v) = 2\pi \Delta n \left[\frac{d(b_A V)}{dV} - \frac{d(b_S V)}{dV} \right] \Delta v. \tag{5}$$

Using the measured values of $\Delta \nu$ for the three cases described in Sec. III and determining for each $\Delta \nu$ the value of $\Delta k(\Delta \nu)$ from the plot of Fig. 4, we found $f(\Delta \nu)$, to equal $-\Delta k(\Delta \nu)$ in the case of phase matching, in accord with Eq. (3). The differences of the group delays of the different mode pairs, calculated from Eq. (5), are fairly well described, as shown by us earlier,[5] by the theoretical relations obtained in Ref. 7 for the group delays. Thus, investigations of the SFPM turn out to provide information in the analysis of group delays in optical wave guides, a fact of great practical interest.

2. SFPP with large frequency shifts (Fig. 3)

We consider the case of generation of Stokes–anti-Stokes pairs shown in Fig. 3 (A_1–S_1). For the two investigated optic waveguides, generation was ob-

served of two Stokes–anti-Stokes pairs corresponding to LP_{11} modes, with the direction of the lobes of one Stokes–anti-Stokes pair perpendicular to that of the lobes of the other pair. Generation of two such pairs is due to the difference between the propagation constants of LP_{11} modes with orthogonal lobe direction. This question will be considered in greater detail in Sec. V.

An analysis of Eq. (4) shows that at such considerable frequency shifts $\Delta \nu$, in the case when the photons propagate at the Stokes and anti-Stokes frequencies in the LP_{11} mode, two cases are possible: 1) both pump photons in the LP_{01} mode, and 2) one pump photons in the LP_{01} mode and the other in the LP_{11} mode. The second case, however, is not realistic, since the overlap integral of the fields of the four linearly polarized modes that participate in the process is zero in this situation.[2] For the first case, $f(\Delta \nu)$, as follows from (2), takes the form

$$f(\Delta v) = 2\pi \Delta n (b_{11} v_S + b_{11} v_A - 2 b_{01} v_p). \tag{6}$$

Recognizing that the dispersion characteristic of the LP_{11} mode remains practically unchanged for the refractive-index profiles shown in Fig. 2, we can calculate the normalized propagation constant b_{01} from the measured frequency shifts $\Delta \nu$. From Eqs. (6) and (3) we have

$$b_{01} = [2\pi \Delta n (b_{11} v_S + b_{11} v_A) + \Delta k(\Delta v)]/4\pi \Delta n v_p. \tag{7}$$

ν_S and ν_A were measured in the experiment, $\Delta k(\Delta \nu)$ was determined from the plot of Fig. 4 using the measured $\Delta \nu$, and the values of b_{11} were determined from the theoretical data[7] (Fig. 2) for an optical waveguide with a steplike refractive-index profile. Figure 2 show the values of b_{01} obtained in this manner for waveguides 1 and 2. It is seen that the dispersion of the LP_{01} modes of the investigated optic waveguides differs substantially from the dispersion of waveguides with a steplike refractive-index profile. The presence of a large number of optic waveguides with different core diameters, obtained from one stock piece, makes it possible to reconstruct the dispersion characteristics more fully. The capabilities of the method are extended also by the use of frequency-tuned pumping lasers. We note that knowledge of the dispersion characteristics of optic waveguides is not only of scientific, but also of practical interest when it comes to developing new optic waveguides.

V. FREQUENCY SPLITTING OF LP_{11} MODES IN SFPP (FIG. 3)

To ascertain the causes of generation of two pairs of LP_{11} modes in the investigated optic waveguides (Fig. 3) we use the following reasoning. We have used above the concept of linearly polarized modes, which are the solutions of a scalar wave equation with circular symmetry in the approximation $\Delta n = 0$ (Ref. 11). In this approximation, the symbol LP_{lm} with $l \geqslant 1$ stands for four modes with identical propagation constants β: two orthogonal polarizations, each of which has an angular dependence $\cos l\varphi$ (even) and $\sin l\varphi$ (odd symmetry).

For a circularly symmetrical optic waveguide, the

LP_{lm} are "pseudomodes," since they are linear combinations of the elementary $HE_{l+1,m}$- and $EH_{l-1,m}$- modes that have different β and furthermore are inhomogeneously polarized. In particular, the LP_{11} modes of interest to us consist of even-symmetry modes $EH_{01} = TM_{01}$ and odd-symmetry modes $EH_{01} = TE_{01}$ and HE_{21}. These HE and EH modes are the true modes of an optic waveguide with circular symmetry. Therefore, the higher-order LP_{lm} modes are not stable, i.e., as they propagate through the waveguide they can change both in configuration and in polarization. Thus, for example, by virtue of the difference between the propagation constants of the modes HE_{21} and EH_{01}, the LP_{11} mode with even symmetry and with homogeneous polarization directed along the lobes is transformed after a period

$$L = \pi/(\beta_{HE_{21}} - \beta_{EH_{01}})$$

into an LP_{11} mode with odd symmetry and with polarization orthogonal to the initial mode. If the difference $\beta_{EH} - \beta_{HE} \to 0$, and consequently the beat period $L \to \infty$, a stable LP mode will propagate in the optic waveguide.

Real waveguides differ in practice, to a greater or lesser degree, from waveguides having circular symmetry, i.e., they have elliptic cores. The optic waveguides with circular elliptic symmetry have different mode fields. The mode fields in an elliptic optic waveguide can be represented as fields of transformed modes of a waveguide with circular symmetry. In this case, the fields of the elliptic waveguide mode are linear combinations of two even- and odd-symmetry LP_{lm} modes of a waveguide having different propagation constants β_e (even-symmetry) and β_o (odd-symmetry). The constants β_e and β_o are obtained by solving the scalar wave equation in elliptic geometry and in the approximation $\Delta n = 0$.

To facilitate the mode analysis in a real elliptic waveguide, it was proposed in Ref. 11 to introduce the parameter

$$\Lambda = (\beta_e - \beta_o)/(\beta_{EH} - \beta_{HE})$$

(β_{EH} and β_{HE} are the propagation constants of the corresponding EH and HE modes in a waveguide with circular symmetry). When the parameter $\Lambda \gg 1$, a stable LP_{lm} ($l \geq 1$) mode will propagate in the optic waveguide; conversely, it is impossible to speak of LP modes in optic waveguides if $\Lambda \ll 1$. In a waveguide with sufficient ellipticity, modes of unlike parity have substantially different β, while modes of like parity have close values of β.

In the optic waveguides investigated by us the LP_{lm} modes are stable. This is seen (see Fig. 3) using as an example an LP_{11} modes consisting of a pair of distinctively separated lobes. If the LP_{11} mode were unstable, its near field would be a ring.[2] Evidence of the stability of the LP_{11} mode in our case is also the fact that the LP_{11} mode in optic waveguide No. 1 of ~1 m length, at a definite azimuth of the linear polarization on entering the waveguide (we used laser radiation with $\lambda = 1.064$ μm), was linearly polarized to a high degree.

Thus, we attribute the generation of two pairs of LP_{11}

TABLE I.

GFOW	$\Delta\nu_1$, cm^{-1}	$\Delta\nu_2$, cm^{-1}	$\beta_e - \beta_o$, cm^{-1}	e^2	Λ_1	Λ_2
№ 1 ($a \approx 4.5$ μm)	1950	2100	7.5	0.118	53	135
№ 2 ($a \approx 3.7$ μm)	2600	2800	10.5	0.124	46	178

modes having orthogonal lobe directions (Fig. 3) to the difference between the propagation constants β of LP_{11} modes of unlike symmetry parity, which is the consequence of the ellipticity of the waveguide cross section.

We calculate now the difference between the propagation constants β of these modes and the ellipticity that causes this difference. If the Stokes–anti-Stokes pair with even-symmetry LP_{11} modes is generated with a frequency shift $\Delta\nu_1$, and that with odd-symmetry with $\Delta\nu_2$, then, taking into account expression (6), which we can rewrite in the form

$$f(\Delta\nu) \approx 4\pi \Delta n \nu_{11}(b_{11} - b_{01}),$$

we have

$$f(\Delta\nu_1) - f(\Delta\nu_2) = 4\pi \Delta n \nu_{11}(b_e - b_o) = 2(\beta_e - \beta_o). \tag{8}$$

from the mode locking condition (3) it follows that

$$\beta_e - \beta_o = \tfrac{1}{2}[\Delta k(\Delta\nu_2) - \Delta k(\Delta\nu_1)]. \tag{9}$$

Thus, from the experimentally measured shifts $\Delta\nu_1$ and $\Delta\nu_2$, using the data of the curve on Fig. 4, we can calculate the difference $\beta_e - \beta_o$, knowledge of which enables us in turn, by using Eqs. (38) and (35) of Ref. 11, to calculate the parameter Λ and the ellipticity of the optic waveguide

$$e = (1 - a_1^2/a_2^2)^{1/2}$$

(a_1 and a_2 are the major and minor axes of the ellipse). The values calculated in this manner are summarized in Table I, where we use the notation

$$\Lambda_1 = (\beta_e - \beta_o)/|\beta_{TE_{01}} - \beta_{HE_{21}}|,$$
$$\Lambda_2 = (\beta_e - \beta_o)/|\beta_{TM_{01}} - \beta_{HE_{21}}|.$$

The cross-section ellipticities for the two optic waveguides agree well with the values obtained from the density patterns of the photographed cross section of the waveguide.

VI. BIFERINGENCE IN OPTIC WAVEGUIDES

Another possible cause of generation of two pairs of LP_{11} modes (see Fig. 3) may be birefringence in the optical waveguides,[12] namely the difference between the propagation constants of two LP modes having orthogonal polarization. We have suggested this possibility in our preceding paper.[5] To estimate the contribution of the birefringence and the observed splitting of the LP_{11} modes in SFPP we measured the birefringence in the optic waveguide No. 2. A laser with $\lambda = 1.064$ μm excited in the optic waveguide a fundamental LP_{01} mode and the birefringence was measured with a $\lambda/4$ plate and with analyzing A (see Fig. 1) using the procedure described in Ref. 12. The measured birefringence, corresponding to a difference between the propagation constants of orthogonally polarized LP_{01} modes, turned out to be $\Delta\beta = 0.01$ cm^{-1}. It can be assumed that the

birefringence for the LP_{11} mode will not differ significantly from that measured for the LP_{01} mode.

As seen from the data in Table I, the measured birefringence leads to a difference $\Delta\beta$ between the propagation constants that is several orders smaller than measured from the SFPP data. We note that in principle it is possible to produce optic waveguides with strong birefringence that leads to $\Delta\beta \sim 10$ cm^{-1} (see Ref. 12 and the bibliography therein).

The birefringence measured by us for the optic waveguide No. 2 agrees with good accuracy with the value obtained from the following expression of Marcuse (see Ref. 13) with allowance for the ellipticity e given in Table I:

$$\Delta\beta = \frac{e^2\theta_c^3 U^2 W^2}{8aV^3}, \qquad \theta_c = \left(1 - \frac{n_2^2}{n_1^2}\right)^{1/2};\qquad (10)$$

here θ_c is the critical angle, U is the radial phase parameter inside the core, and W is the radial damping parameter in the cladding.[6] It should be noted that this formula does not take into account the birefringence due to the anisotropic stresses in the optic waveguide, which should be quite small in the waveguides investigated by us.[12]

Thus, the generation of Stokes–anti-Stokes pairs observed by us in GFOW has been explained within the framework of four-photon mixing, with the interacting-wave mode-locking conditions satisfied. Generation of Stokes–anti-Stokes pairs with a maximum frequency shift ~ 5500 cm^{-1} was obtained. The possibility of varying the optic-waveguide parameters, for example the diameter of the core and the difference between the refractive indices of the core and of the cladding make it possible to obtain a source of tunable laser radiation in a wide spectral range. The use of a frequency-tunable pumping laser is apparently particularly promising for conversion of the radiation frequency into the near-infrared (1–1.8 μm).

The procedure of investigating four-photon processes yields valuable information on certain properties of optical waveguides. In this paper we have proposed and demonstrated a method of measuring the dispersion characteristics of optic waveguides. The method is convenient also for selective excitation of the modes in optic waveguides.

[1] R. H. Stolen, Fiber and Integrated Optics **3**, 21 (1980).

[2] R. H. Stolen, IEEE J. QE **11**, 100 (1975).

[3] K. O. Hill, D. C. Johnson, and B. S. Kawasaki, Appl. Opt. **20**, 1075 (1981).

[4] Chinlon Lin and M. A. Bosh, Appl. Phys. Lett. **38**, 479 (1981).

[5] E. M. Dianov, E. A. Zakhidov, A. Ya. Karasik, P. V. Mamyshev, and A. M. Prokhorov, Pis'ma Zh. Eksp. Teor. Fiz. **34**, 40 (1981) [JETP Lett. **34**, 38 (1981)].

[6] D. Gloge, Appl. Opt. **10**, 2252 (1971).

[7] R. H. Stolen, Appl. Opt. **14**, 1533 (1975).

[8] Y. R. Shen and N. Bloembergen, Phys. Rev. **A137**, 1787 (1965).

[9] A. B. Grudinin, A. M. Gur'yanov, E. M. Dianov, É. A. Zakhidov, A. Ya. Karasik, and A. V. Luchnikov, Kvant. Elektron. (Moscow) **8**, 2383 (1981) [Sov. J. Quantum Electron. **11**, 1456 (1981)].

[10] A. V. Belov, A. N. Gur'yanov, E. M. Dianov, V. M. Mashinskii, V. B. Neustruev, A. V. Nikolaichik, and A. S. Yushin, *ibid.* **5**, 695 (1978) [**8**, 410 (1978)].

[11] S. W. Synder and W. R. Young, Opt. Soc. Am. **68**, 297 (1978).

[12] A. N. Gur'yanov, L. D. Gusovskii, G. G. Devyatykh, E. M. Dianov, A. P. Karasik, V. A. Kozlov, M. M. Mirakyan, and A. M. Prokhorov, Kvant. Elektron. (Moscow) **8**, 2473 (1981) [Sov. J. Quantum Electron. **11**, 1509 (1981)].

[13] M. J. Adams, D. N. Payne, and C. M. Ragdale, Electron. Lett. **15**, 298 (1979).

Translated by J. G. Adashko